

The Atomic-Scale Magnetism of Co₂FeAl Heusler Alloy Epitaxial Thin Films

Xiaoqian Zhang,^{1,b)} Wenqing Liu,^{1,2,3,b)} Yu Yan,³ Wei Niu,^{1,4} Bolin Lai,¹ Yafei Zhao,¹
Wei Wang,¹ Liang He,^{1,a)} Hao Meng,⁵ Yongbing Xu^{1,3,a)}

¹*Jiangsu Provincial Key Laboratory of Advanced Photonic and Electronic Materials, Collaborative Innovation Center of Advanced Microstructures, School of Electronic Science and Engineering, Nanjing University, Nanjing 210093, China*

²*Department of Electronic Engineering Royal Holloway University of London Egham, Egham, Surrey TW20 0EX, UK*

³*York-Nanjing Joint Centre (YNJC) for spintronics and nano engineering, Department of Electronic Engineerings, The University of York, YO10 3DD, United Kingdom*

⁴*School of Science, Nanjing University of Posts and Telecommunications, Nanjing 210023, China*

⁵*Zhejiang Hikstor Technology Company, Hangzhou 311305, China*

^{b)} Xiaoqian Zhang and Wenqing Liu contributed equally to this work.

ABSTRACT

The atomic-scale magnetism of Co₂FeAl Heusler Alloy has long been an outstanding question, and with the thickness down to nanometer scale, this become even more sophisticated. Here we report a direct measurement of the Co₂FeAl epitaxial thin films on the GaAs(001) substrate with *in-situ* magneto-optic Kerr effect (MOKE) and the synchrotron-based X-ray magnetic circular dichroism (XMCD) techniques. Strong uniaxial magnetic anisotropy (UMA) have been observed from all thicknesses of the Co₂FeAl thin films between 3 unit cells (uc) and 20 uc. A critical thickness of 3 uc has been identified, below which an anti-parallel spin component of the Co atoms occur. This anti-parallel spin component can be responsible for the significantly reduced magnetic moment and the low spin-polarization near the Fermi level of the Co₂FeAl.

Spintronics is one of the new fields with high potential for practical applications,¹ after the discovery of the giant magnetoresistance² and the tunneling magnetoresistance effect.^{3,4} The realization of spin transport at the interface of semiconductor and magnetic materials is the key building block for spintronic devices.⁵⁻⁷ As a standard prototype to explore ferromagnetic/semiconductor interfaces, Co₂FeAl/GaAs heterostructure has attracted a lot of attention, because Co₂FeAl possesses high spin polarization,⁸ low damping coefficient,⁹ and small lattice mismatch with GaAs substrate.

In our previous report, we have found a linear relationship of thickness dependent magnetization with a critical thickness of 4 unit cells (uc) (1 uc = 0.573 nm) in the Co₂FeAl/GaAs system,¹⁰ below which the magnetization decreases rapidly. This phenomenon has also been found in similar systems such as Co₂Cr_{0.6}Fe_{0.4}Al¹¹ and Co₂FeSi.¹² Lower magnetization of ultra-thin films hinders their applications in spintronic devices, thus a fundamental understanding on magnetic configuration of the ultra-thin Co₂FeAl film is crucial.

In this work, Co₂FeAl films grown on GaAs(001) substrate with thicknesses of 3 uc, 5 uc and 20 uc were studied. X-ray absorption spectroscopy (XAS) and X-ray magnetic circular dichroism (XMCD) techniques have been used to probe the element-specific magnetic moment. An anti-parallel spin component of Co with a thickness of 3 uc at the interface was firstly observed, which explains the abrupt decrease of magnetization below the critical thickness. For the films thicker than ~ 3 uc, they possess the bulk magnetization, accompanied by parallel alignment of both Fe and Co atoms.

Co₂FeAl ultra-thin films were epitaxially grown on GaAs substrates by molecular beam epitaxy (MBE). The detailed growth method can be found in our previous work.¹⁰ The as-

grown single-crystalline Co_2FeAl film was evidenced by *in-situ* reflection high energy electron diffraction (RHEED) patterns [Fig. 1(a)-1(b)], with Co_2FeAl (001)[110] // GaAs (001)[110]. B2 structure was demonstrated by X-ray diffraction characterization in the former report.¹⁰ In this structure, Co atoms occupy the eight vertexes of the primitive cube, and Fe and Al atoms sit at the center of the cube, randomly [Fig. 1(c)]. After the growth, Co_2FeAl thin films were capped with a 2-nm-thick Al layer to prevent oxidation in air.¹³ Figure 1(d) exhibits the magnetic hysteresis loops of Co_2FeAl (001) thin films of different thicknesses measured by vibrating sample magnetometer (VSM) at 300 K. For the 20-uc-thick film, the presence of a bulk-like magnetization ($\sim 5.28 \mu_B/\text{f.u.}$) was identified.¹⁴⁻¹⁷ However, as the thickness decreases, the magnetization decreases to $2.92 \mu_B/\text{f.u.}$ at 5 uc and $1.16 \mu_B/\text{f.u.}$ at 3uc.

To acquire a more comprehensive magnetism of the Co_2FeAl thin films, the magnetic hysteresis loops were collected using *in-situ* magneto-optic Kerr effect (MOKE)⁶ set-up at room temperature immediately after the growth, as exhibited in Fig. 2. Longitudinal Kerr rotation was measured using an electromagnet with the largest field of 500 Oe, and an intensity stabilized HeNe laser (633 nm).¹⁸ Magnetic hysteresis loops were swept in plane with a rotation step of 15 degrees. Square loops are observed when the field is applied along the $[1 \bar{1} 0]$ direction, which is the easy axis. On the contrary, the hard axis is along $[1 1 0]$. The polar plot of the measured Kerr rotation at zero field is revealed in Fig. 2(j). The films clearly display an in-plane uniaxial anisotropy, which is opposite to the four-fold symmetry of the bulk.¹⁹ This is mostly caused by the bonds between As and Co atoms [Fig. 1(c)] at the interface.^{6,20} The GaAs(001) surface has Ga dimers along $[110]$ and As dimers along $[1 \bar{1} 0]$, which degenerates the four-fold symmetry into a two-fold symmetry. And as Co atoms

prefer to bind with As atoms,¹¹ Co chains are formed along $[1\bar{1}0]$. Thus the uniaxial anisotropy of Co₂FeAl thin films suggests that the properties of ultra-thin films are influenced by the interface dramatically.

To determine the magnetic and electronic structure of Co₂FeAl epitaxial thin films, the element-specific technique of XAS and XMCD at Co and Fe $L_{2,3}$ absorption edges were performed at beamline I06 of Diamond Light Source in U.K.^{21,22} The light-helicity was switched in a saturated magnetic field of 1 T, which was applied in parallel with the incident beam and at 60 degrees with respect to the film plane.²³ The spectra were recorded using the total electron yield (TEY) method at 300 K. XMCD was obtained by taking the difference of the XAS spectra, $\sigma - \bar{\sigma}$, where σ represents the TEY-XAS intensities for respective helicities of the emitted light. Typical XAS and XMCD spectra of Co₂FeAl films at Co and Fe $L_{2,3}$ edge are presented in Fig. 3. It shows a white line at each spin-orbit split core level without prominent splitting for both left- and right-circularly polarized X-rays, indicating that samples have been well protected from oxidation.^{24,25} The shoulder structures (light blue arrows) appearing in the higher photon energy region of Co L_3 peaks is due to the Co-Co bonding states. This suggests that most Co atoms sit at the proper sites (the apexes of the cube). On the contrary, no observable shoulders for Fe indicates that most Fe atoms sit randomly in the center of the cube, as shown in Fig. 1(c). This is consistent with B2 structure.^{14,26}

The intensities of XAS for all the samples have been normalized for comparison. As shown in Fig. 3, the XMCD signals decrease with film thickness reducing. For the thickness of 20 uc and 5 uc, XMCD spectra of both Co and Fe don't split, which indicates a ferromagnetic coupling within Co atoms and Fe atoms. Meanwhile, XMCD spectra of Co

and Fe point to the same direction, demonstrating these two elements are ferromagnetically coupled.¹⁵ When the thickness reduces to 3 uc, there is a positive and negative peak of 777.3 eV and 778.5 eV at L_3 edge of Co [Fig. 3(d)]. The observation of this multiplet structure is indicative of opposite alignment of spins for Co atoms (pink line). For Fe atoms, only decreased intensity of XMCD spectrum with no splitting suggests the suppressed magnetization of Fe. This result demonstrates that the interface with weak magnetization is caused by the anti-parallel spin component of Co atoms and magnetization-suppressed Fe atoms. The net magnetic moments of Co and Fe point to the same direction, indicating the ferromagnetic coupling between Co and Fe.

It must be mentioned that the split of the XMCD spectrum is distinct from the disordered arrangement of magnetism, which only leads to the decrease of the peak (valley). The spectral splitting observed here is definitely related to the anti-parallel spin arrangement of Co atoms.²⁷

Using the sum rule analysis, we have extracted the spin and orbital magnetic moments from the XMCD spectra. At the $L_{2,3}$ edges of Co and Fe, $2p$ core electrons are excited into unoccupied $3d$ states, allowing us to directly investigate the magnetically polarized $3d$ band. The spin (m_s) and orbital (m_l) moments of Co and Fe were calculated according to equations:

$$m_l = -\frac{4qn_h}{3rp \cos \theta} \quad (1)$$

$$m_s = \frac{(4q-6p)n_h}{rp \cos \theta} \quad (2)$$

The values of the parameters p , q , and r derived from the integrals of the XMCD and XAS spectra in the manner of Chen *et al.*²⁵ The number of $3d$ holes, n_h , were taken to be 2.5 for Co and 3.4 for Fe based on the work of H. J. Elmers.^{28,29}

Table 1 summarizes the obtained element-specific magnetic moment of our samples and some of the experimental and theoretical efforts from the literature. In the 20-uc-thick sample, the total magnetic moment has been evaluated as $5.86 \pm 0.1 \mu_B/\text{f.u.}$, similar to $6.22 \mu_B/\text{f.u.}$ reported by K. K. Meng *et al.*^{30,31} And this number is very close to the previous value of $5.28 \mu_B/\text{f.u.}$ measured by VSM [Fig. 1(d)]. The slight lower value measured by VSM is because VSM measures the average value of the whole film which includes the weak magnetized layer at the interface.³² In the surface-sensitive TEY mode, the obtained electrons are mostly from the top surface with an exponential attenuation ($\exp(-x/\lambda_e)$, $\lambda_e \sim 3$ nm) into the bulk.^{21,22} The obtained signal is from the top few layers. Therefore, for a 20-uc-thick film, the measured magnetization is bulk-like. Our value is larger than the theoretical value of $5 \mu_B/\text{f.u.}$ ^{16,33,34} with $L2_1$ structure, which is thought to occur due to a smaller higher concentration of Fe, which replaces small fraction of Co in the film, for the magnetic moment of Fe atoms ($\sim 2.6 \mu_B$) is higher than the Co atoms ($\sim 1.7 \mu_B$).³⁰

As the thickness decreases to 5 and 3 uc, the total magnetic moment also shrinks to $3.25 \mu_B/\text{f.u.}$ and $0.93 \mu_B/\text{f.u.}$ (top three lines of the table), respectively, consistent with previous VSM results [Fig. 1(d)]. The presence of oxidation in thinner films can be ruled out for the absence of oxidation peak in XAS spectra.¹⁵ The deviation of magnetic moments of epitaxial thin films from the bulk is usually attributed to multiple reasons. The first one is the interfacial diffusion, which are As and Al atoms in this case. The substitution of As would

only happen at the first 1-2 atomic layers at the interfaces. To exclude possibility of diffusion of As, the interfacial layer with weak magnetization is calculated. Considering the exponential attenuation of electrons from the top surface into bulk in TEY mode, the average magnetization of 5-uc-thick Co_2FeAl film composed of 3-uc-thick interfacial layer is calculated to be $3.41 \mu_B/\text{f.u.}$, which is very close to the value we measured ($3.25 \mu_B/\text{f.u.}$). However, 3 uc is much thicker than 1-2 atomic layers. Y. K. Takahashi *et al.*³⁵ and Z. Wen *et al.*³⁶ have demonstrated that the diffusion length of Al at the interface is about 1 nm by STEM (scanning transmission electron microscopy), which is close to the critical thickness we measured. They have found that diffusion of Al into the substrate can alter the electronic structure and magnetic damping Co_2FeAl layer at the interface. Non-compensation occurs due to broken symmetry of magnetite at the interface, is the second mechanism. K.K. Meng *et al.*³⁷ reported the formation of completely disordered A2 structure with decreasing the thickness of Co_2FeAl due to interfacial stress and the vanished Berry curvature. In consistence with the mentioned results, we obtained the dramatically dropped spin moments of Co and Fe atoms with films thickness decreasing, which is related to the antiparallel coupled Co atoms and magnetic suppression of Fe atoms. It may be resulted from the diffusion of Al and the broken symmetry at the interface.

Distinguished from other ordinary magnetic materials, the Co-Fe exchange interactions are much stronger than Co-Co/Fe-Fe,³⁸ and there exists charge transfer between Co and Fe atoms. Remarkably, Jaw-Yeu Liang *et al.*³⁹ suggested that the magnetic properties of Co_2FeAl is dominated by Co-Fe exchange correlation by the view point of the spin electronic states. The transferring electrons from Co minority states to Fe minority states, induce the enhancement of the magnetization and spin polarization of Co, at the expense of Fe. The

much suppressed magnetization of Fe we obtained shows good agreement with this finding. However, this charge transfer effect induces an anti-parallel spin alignment of Co in 3-uc-thick film, which greatly reduced the net magnetization of Co_2FeAl .

The magnetic ordering of Co_2FeAl thin film is schematically sketched in Fig. 4. The yellow and green area represents the interfacial layer and the bulk state, respectively. In the interfacial layer, Co atoms are antiparallel coupled with each other, and the magnetization of Fe is suppressed, which may come from the charge transfer effect, the diffusion of Al and broken symmetry at the interface. It reduces the magnetization and spin polarization enormously. For the films thicker than 3 uc, both Fe and Co atoms are ferromagnetically coupled, and the magnetization reaches the bulk value.

To summarize, we have performed a comprehensive study of Co_2FeAl thin films with different thicknesses epitaxially grown on GaAs(001) substrates. High quality of XAS and XMCD spectra were obtained and analyzed using the sum rules. The interfacial layer (~ 3 uc) with weak magnetization is verified to be caused by the anti-parallel spin component between Co atoms and magnetic suppression within Fe atoms. It may come from the charge transfer effect, diffusion of Al and broken symmetry at the interface, which also induces the in-plane uniaxial magnetic anisotropy characterized by *in-situ* MOKE measurements. Above the critical thickness, all the atoms are ferromagnetically coupled. Our findings offer evidence of the existence of anti-parallel spin arrangement of Co atoms and charge transfer between Co and Fe at the interface of $\text{Co}_2\text{FeAl}/\text{GaAs}$ system firstly. Besides, it explains the low spin injection efficiency^{40,41} and spin polarization values¹⁰ previously found in this heterostructure, which is essential for spintronics applications.

Acknowledgements

This work is supported by the National Key Research and Development Program of China (No. 2016YFA0300803, No. 2017YFA0206304), the National Basic Research Program of China (No. 2014CB921101), the National Natural Science Foundation of China (No. 61427812, 11774160, 11574137, 61474061, 61674079), Jiangsu Shuangchuang Program, the Natural Science Foundation of Jiangsu Province of China (No. BK20140054) and UK EPSRC (EP/S010246/1). Diamond Light Source is acknowledged to I06 under proposal SI17930.

References

- 1 S. A. Wolf, D. D. Awschalom, R. A. Buhrman, J. M. Daughton, S. von Molnar, M. L. Roukes,
A. Y. Chtchelkanova, and D. M. Treger, *Science* **294**, 1488 (2001).
- 2 S. Yuasa, T. Nagahama, A. Fukushima, Y. Suzuki, and K. Ando, *Nat. Mater.* **3** (12), 868 (2004).
- 3 T. Kimura, Y. Tomioka, H. Kuwahara, A. Asamitsu, M. Tamura, and Y. Tokura, *Science* **274**,
1698 (1996).
- 4 S. S. Parkin, C. Kaiser, A. Panchula, P. M. Rice, B. Hughes, M. Samant, and S. H. Yang, *Nat.*
Mater. **3** (12), 862 (2004).
- 5 J. S. Claydon, Y. B. Xu, M. Tselepi, J. A. Bland, and G. van der Laan, *Phys. Rev. Lett.* **93** (3),
037206 (2004).
- 6 Y. B. Xu, E. T. M. Kernohan, D. J. Freeland, A. Ercole, M. Tselepi, and J. A. C. Bland, *Phys. Rev.*
B **58**, 890 (1998).
- 7 Kazutaka Nagao, Yoshio Miura, and Masafumi Shirai, *Phys. Rev. B* **73** (10), 104447 (2006).
- 8 Wenhong Wang, Hiroaki Sukegawa, Rong Shan, Seiji Mitani, and Koichiro Inomata, *Appl.*
Phys. Lett. **95** (18), 182502 (2009).
- 9 S. Mizukami, D. Watanabe, M. Oogane, Y. Ando, Y. Miura, M. Shirai, and T. Miyazaki, *J. Appl.*
Phys. **105** (7), 07D306 (2009).
- 10 X. Zhang, H. Xu, B. Lai, Q. Lu, X. Lu, Y. Chen, W. Niu, C. Gu, W. Liu, X. Wang, C. Liu, Y. Nie, L.
He, and Y. Xu, *Sci. Rep.* **8** (1), 8074 (2018).
- 11 A. Hirohata, M. Kikuchi, N. Tezuka, K. Inomata, J. Claydon, Y. Xu, and G. Vanderlaan, *Current*
Opinion in Solid State and Materials Science **10** (2), 93 (2006).
- 12 H. Schneider, G. Jakob, M. Kallmayer, H. J. Elmers, M. Cinchetti, B. Balke, S. Wurmehl, C.
Felsler, M. Aeschlimann, and H. Adrian, *Phys. Rev. B* **74**, 174426 (2006).
- 13 Murong Lang, Liang He, Faxian Xiu, and Xinxin Yu, *ACS nano* **6** (1), 295 (2012).
- 14 I. Galanakis, P. H. Dederichs, and N. Papanikolaou, *Phys. Rev. B* **66** (17), 174429 (2002).
- 15 S. Soni, S. Dalela, S. S. Sharma, E. K. Liu, W. H. Wang, G. H. Wu, M. Kumar, and K. B. Garg, *J.*
Alloys Comp. **674**, 295 (2016).
- 16 SH Nie, YY Chin, WQ Liu, JC Tung, J Lu, HJ Lin, GY Guo, KK Meng, L Chen, and LJ Zhu, *Phys.*
Rev. Lett. **111**, 027203 (2013).
- 17 Mohamed Belmeguenai, Hanife Tuzcuoglu, Mihai Gabor, Traian Petrisor, Coriolan Tiusan,
Dominique Berling, Fatih Zighem, and Salim Mourad Chérif, *J. Magn. Magn. Mater.* **373**, 140
(2015).
- 18 W. H. Wang, M. Przybylski, W. Kuch, L. I. Chelaru, J. Wang, Y. F. Lu, J. Barthel, H. L.
Meyerheim, and J. Kirschner, *Phys. Rev. B* **71** (14), 144416 (2005).
- 19 M. S. Gabor, T. Petrisor, C. Tiusan, M. Hehn, and T. Petrisor, *Phys. Rev. B* **84** (13), 134413
(2011).
- 20 Simon Trudel, Georg Wolf, Jaroslav Hamrle, Burkard Hillebrands, Peter Klaer, Michael
Kallmayer, Hans-Joachim Elmers, Hiroaki Sukegawa, Wenhong Wang, and Koichiro Inomata,
Phys. Rev. B **83** (10), 104412 (2011).
- 21 Wenqing Liu, Damien West, Liang He, Yongbing Xu, Jun Liu, Kejie Wang, and Yong Wang,
ACS nano **9**, 10237 (2015).
- 22 W. Liu, L. He, Y. Xu, K. Murata, M. C. Onbasli, M. Lang, N. J. Maltby, S. Li, X. Wang, C. A. Ross,
P. Bencok, G. van der Laan, R. Zhang, and K. L. Wang, *Nano Lett.* **15** (1), 764 (2015).
- 23 W. Liu, Q. Zhou, Q. Chen, D. Niu, Y. Zhou, Y. Xu, R. Zhang, J. Wang, and G. van der Laan, *ACS*
Appl. Mater. Interfaces **8** (9), 5752 (2016).

- 24 Jill S. Claydon, Sameh Hassan, Christian D. Damsgaard, Jørn Bindslev Hansen, Claus S.
Jacobsen, Yongbing B. Xu, and Gerrit van der Laan, *J. Appl. Phys.* **101** (9), 09J506 (2007).
- 25 C. T. Chen, Y. U. Idzerda, H. Lin, N. V. Smith, G. Meigs, E. Chaban, G. H. Ho, E. Pellegrin, and F.
Sette, *Phys. Rev. Lett.* **75**, 152 (1995).
- 26 I. Galanakis, *Phys. Rev. B* **71**, 012413 (2005).
- 27 P. Gambardella, S. S. Dhesi, S. Gardonio, C. Grazioli, P. Ohresser, and C. Carbone, *Phys. Rev.*
Lett. **88** (4), 047202 (2002).
- 28 H. J. Elmers, G. H. Fecher, D. Valdaitsev, S. A. Nepijko, A. Gloskovskii, G. Jakob, G.
Schönhense, S. Wurmehl, T. Block, C. Felser, P. C. Hsu, W. L. Tsai, and S. Cramm, *Phys. Rev.*
B **67** (10), 104412 (2003).
- 29 H. J. Elmers, S. Wurmehl, G. H. Fecher, G. Jakob, C. Felser, and G. Schönhense, *Appl. Phys. A*
79 (3), 557 (2004).
- 30 K. K. Meng, S. H. Nie, X. Z. Yu, S. L. Wang, W. S. Yan, and J. H. Zhao, *J. Appl. Phys.* **110** (9),
093904 (2011).
- 31 K. K. Meng, S. L. Wang, P. F. Xu, L. Chen, W. S. Yan, and J. H. Zhao, *Appl. Phys. Lett.* **97** (23),
232506 (2010).
- 32 E. Arbelo Jorge, M. Jourdan, M. Kallmayer, P. Klaer, and H. J. Elmers, *J. Phys.: Conf. Ser.* **200**
(7), 072006 (2010).
- 33 T. M. Nakatani, A. Rajanikanth, Z. Gercsi, Y. K. Takahashi, K. Inomata, and K. Hono, *J. Appl.*
Phys. **102** (3), 033916 (2007).
- 34 Ting Huang, Xiao-min Cheng, Xia-wei Guan, and Xiang-shui Miao, *IEEE Trans. Magn.* **51** (11),
1 (2015).
- 35 Y. K. Takahashi, Y. Miura, R. Choi, T. Ohkubo, Z. C. Wen, K. Ishioka, R. Mandal, R. Medapalli,
H. Sukegawa, S. Mitani, E. E. Fullerton, and K. Hono, *Appl. Phys. Lett.* **110**, 252409 (2017).
- 36 Zhenchao Wen, Jason Paul Hadorn, Jun Okabayashi, Hiroaki Sukegawa, Tadakatsu Ohkubo,
Koichiro Inomata, Seiji Mitani, and Kazuhiro Hono, *Appl. Phys. Express* **10**, 013003 (2017).
- 37 K. K. Meng, J. Miao, X. G. Xu, Y. Wu, J. H. Zhao, and Y. Jiang, *Solid State Commun.* **254**, 48
(2017).
- 38 Denis Comtesse, Benjamin Geisler, Peter Entel, Peter Kratzer, and László Szunyogh, *Phys.*
Rev. B **89**, 094410 (2014).
- 39 Jaw-Yeu Liang, Tu-Ngoc Lam, Yan-Cheng Lin, Shu-Jui Chang, Hong-Ji Lin, and Yuan-Chieh
Tseng, *J. Phys. D: Appl. Phys.* **49** (7), 075005 (2016).
- 40 A. Hirohata, H. Kurebayashi, S. Okamura, M. Kikuchi, T. Masaki, T. Nozaki, N. Tezuka, and K.
Inomata, *J. Appl. Phys.* **97** (10), 103714 (2005).
- 41 Zhenchao Wen, Hiroaki Sukegawa, Shinya Kasai, Masamitsu Hayashi, Seiji Mitani, and
Koichiro Inomata, *Appl. Phys. Express* **5** (6), 063003 (2012).

Figure Captions

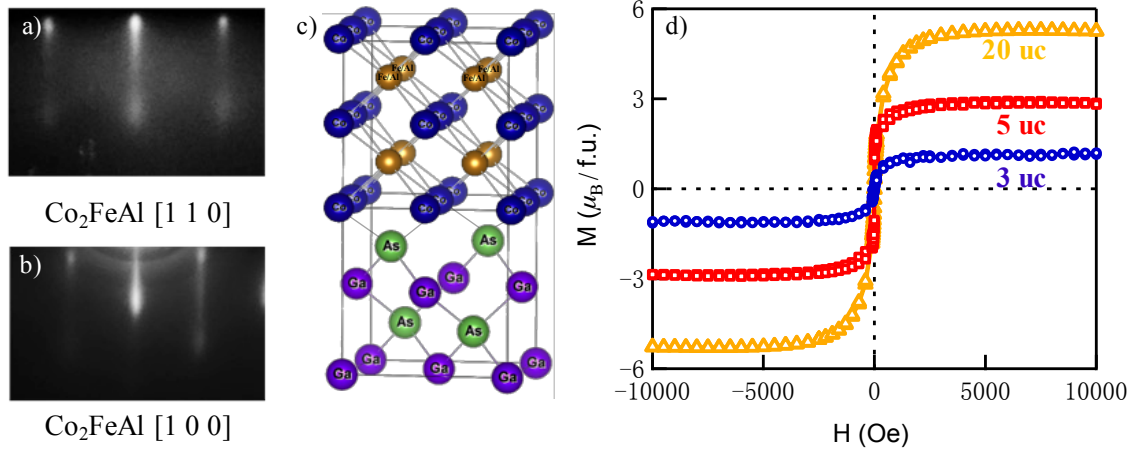


FIG. 1. RHEED and VSM measurements. RHEED patterns of (a)-(b) grown $\text{Co}_2\text{FeAl}(001)$ film with an electron beam along $[110]$ & $[100]$, respectively. (c) Schematic view of $\text{Co}_2\text{FeAl}/\text{GaAs}(001)$ heterostructure. (d) Magnetization of Co_2FeAl films with thickness of 3 uc, 5 uc and 20 uc measured in plane at 300 K.

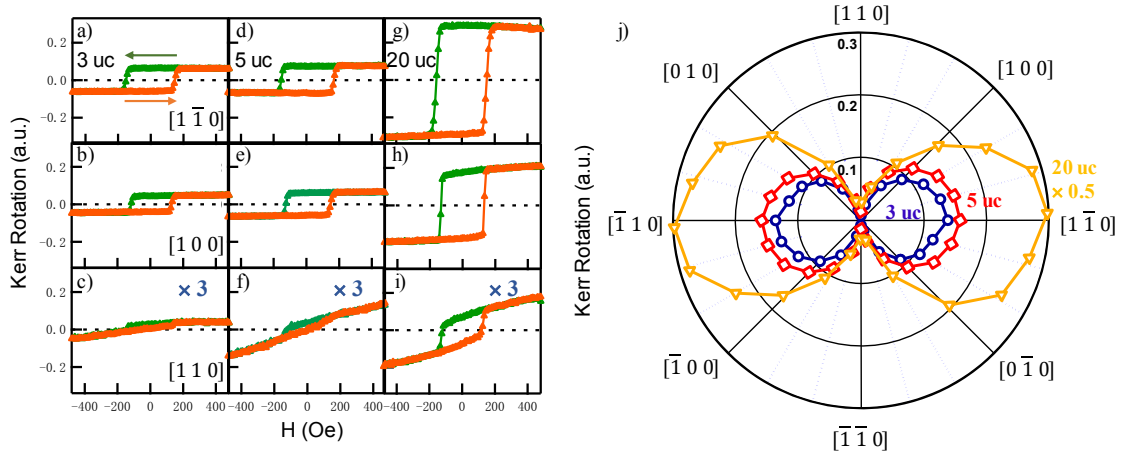


FIG. 2. In-plane uniaxial magnetic anisotropy of Co₂FeAl films by *in-situ* MOKE measurements. Longitudinal Kerr rotation of Co₂FeAl(001) film with thickness of (a)-(c) 3 uc, (d)-(f) 5 uc and (g)-(i) 20 uc measured at 300 K along [1 $\bar{1}$ 0] (easy axis direction), [1 0 0] and [1 1 0], respectively. The orange (green) lines represent that the magnetic field sweeps from negative (positive) to positive (negative). (d) Polar plot of the Kerr rotation for Co₂FeAl(001) films with thickness of 3 uc, 5 uc and 20 uc, which exhibits in-plane uniaxial magnetic anisotropy.

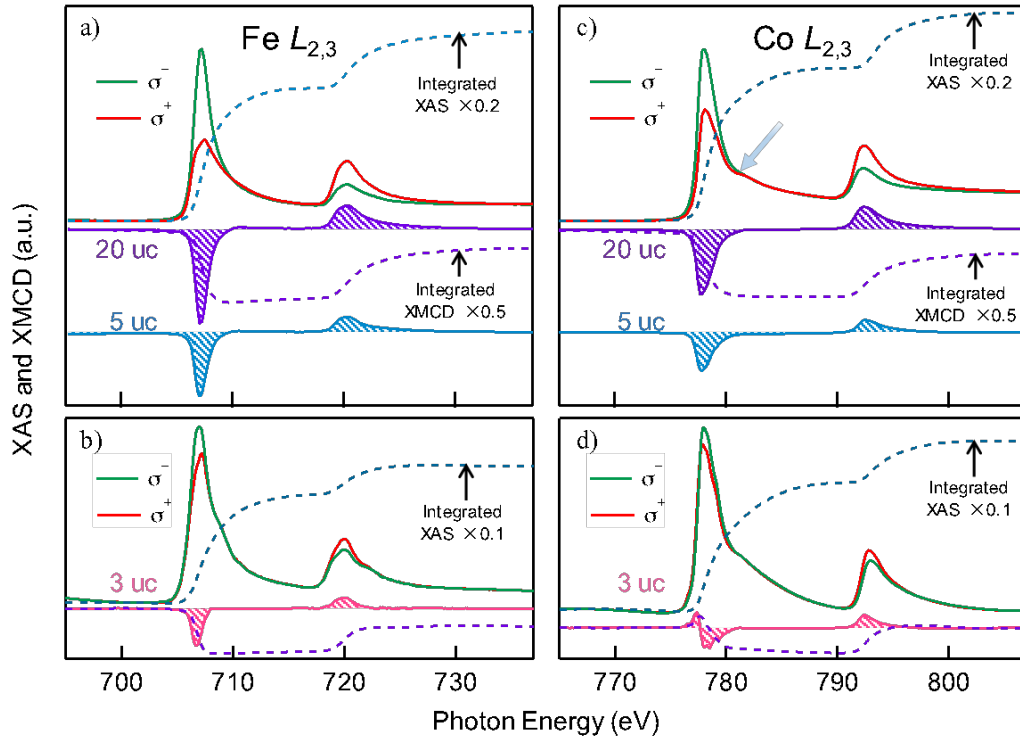


FIG. 3. XAS and XMCD measurements. Typical pairs of XAS and XMCD spectra of (a)-(b) Fe and (c)-(d) Co for Co₂FeAl films with thickness of 20 uc, 5 uc and 3 uc grown on GaAs(001) measured at 300 K. σ^+ and σ^- stand for the XAS probed by left and right X-ray helicities, respectively. The dashed lines represent the integrations of the spectra.

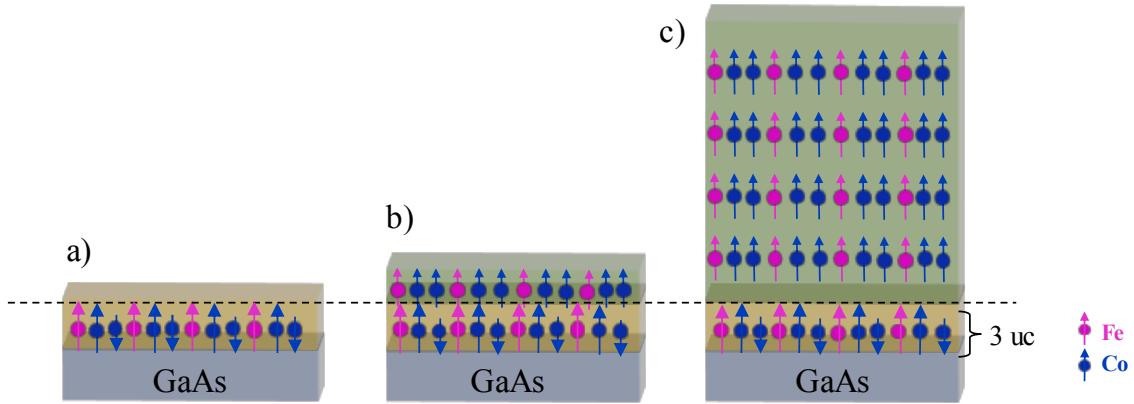


FIG. 4. Schematic diagrams of Co_2FeAl thin films with thicknesses of (a) 3 uc, (b) 5 uc and (c) 20 uc. Yellow area exhibits the interfacial layer with weak magnetization. Green area represents bulk-like ferromagnetic layer.

TABLE I. Spin and orbital moment of our samples and those from the literatures.

Sample	Method	Co ($m_B/f.u.$)	m_{l+s}	Fe m_{l+s} ($m_B/f.u.$)	m_{tot} ($m_B/f.u.$)
20 uc Co ₂ FeAl/GaAs(001)	XMCD	1.66 ± 0.1		2.64 ± 0.1	5.86 ± 0.1
5 uc Co ₂ FeAl/GaAs(001)	XMCD	0.95 ± 0.1		1.45 ± 0.1	3.25 ± 0.1
3 uc Co ₂ FeAl/GaAs(001)	XMCD	0.25 ± 0.05		0.53 ± 0.1	0.93 ± 0.1
7 uc Co ₂ FeAl/GaAs(001) (ref. 30)	SQUID				6.22
9 uc Co ₂ FeAl/GaAs(001) (ref. 37)	XMCD	1.01 ± 0.1		2.18 ± 0.1	4.10 ± 0.1
18 uc Co ₂ FeAl/MgO/Si(001) (ref. 17)	VSM				5.0 ± 0.25
54 uc Co ₂ FeAl/MgO(001) (ref. 15)	XMCD	0.79		2.77	4.25
Single crystal Co ₂ FeAl (ref. 32)	SQUID				4.70
Single crystal Co ₂ FeAl (ref. 32)	XMCD				4.5 ± 0.2
Co ₂ FeAl ingot (ref. 29)	SQUID				5.20
Theory (ref. 33)	GGA+U				5.0
Theory (ref. 34)	LSDA+U	1.24		2.94	4.99